Map-scale folds in Big Brushy Canyon, Northern Sierra del Carmen, Big Bend Region, Texas

Laiza V. Vera-Lopez, Bailey L. Welch, and Joseph I. Satterfield, PhD

Abstract

Detailed, 1:12,000-scale mapping and structural analysis of a 30 km^2 area within northern Sierra del Carmen document two generations of Laramide folds cross-cut by Basin and Range high-angle faults, drag folds, and fault-propagation folds. The Big Brushy Canyon map area falls within the Black Gap Wildlife Management Area, Big Bend National Park, and the Shackelford Ranch. Geologic maps of Moustafa (1988; scale 1:48,000) and St. John (1966; scale 1:62,500) cover this area. Ferrill and others (2004) and Smart and others (2010) described an extensional fault-propagation fold in Big Brushy Canyon. Our mapping will be part of a geologic map of Northern Sierra Del Carmen to be submitted for publication in 2016. Cretaceous rock units exposed include the Del Carmen Limestone, Sue Peaks Formation, Santa Elena Limestone, Del Rio Clay, Buda Limestone, and Boquillas Formation. Tertiary mafic sills intrude the Boquillas Formation. First-phase Laramide folds contain axial planes at 332 85NE (average), fold axes at 327 45 (average), and an average interlimb angle of 52°. Second-phase Laramide folds contain axial planes at 074 90 (average), fold axes at 254 8 (average), and an average interlimb angle of 166°. Third-phase Basin and Range folds, caused by high-angle faults, contain axial planes at 322 64W (average), fold axes of 322 10 (average), and an average interlimb angle of 92°. Four other NW-striking map-scale monoclines have orientations similar to first-phase and third-phase folds and so could be Laramide fault-propagation folds above reverse faults, or Basin and Range fault-propagation folds above normal faults, or both. Folds containing small interlimb angles must be Laramide first-phase folds, while drag folds adjacent to Basin and Range faults must be third-phase folds.

*****

Location and Objectives

The Big Brushy Canyon map area falls within northern Sierra del Carmen in the eastern Big Bend region of Trans-Pecos Texas (Fig. 1). The map area includes the Black Gap Wildlife Management Area, Big Bend National Park, and the Shackelford Ranch. Project objectives are: 1) to construct a detailed, 1:12,000-scale geologic map of the 30 km^2 area (Fig. 2), 2) to describe the orientations and styles of two generations of Laramide folds and one generation of Basin and Range folds, 3) to describe Basin and Range high-angle faults, 4) to document the sequence

of folding and faulting events, and 5) to distinguish contractional fault-propagation folds from extensional fault propagation folds from drag folds. Mapping will be part of a geologic map of northern Sierra Del Carmen to be submitted for publication to the University of Texas Bureau of Economic Geology in 2016.

Methods

This project applied standard techniques of geologic mapping and descriptive structural analysis during three weeks of geologic mapping in and near the map area in August 2014, January 2015 and April 2015. In 2013 - 2014 Bailey Welch mapped an adjacent area to the north in Big Brushy Canyon (Welch and Satterfield, 2014). This project includes his fold data and map unit descriptions. Laiza Vera-Lopez, Travis Williams, Bailey Welch and Joseph Satterfield mapped in two-person teams. To document folds and faults in the area, we measured large numbers of bedding surface orientations with a Brunton compass and plotted on the geologic map (Fig. 2). We distinguished map units by describing rock types, bed thicknesses, and topographic expression. Our descriptions were compared to detailed map unit descriptions in Maxwell et al. (1967) and Moustafa (1988). We located formation contacts by first viewing stereo pairs of aerial photographs, then walking out contacts out or viewing them from a high vantage point. We constructed cross-sections to better understand the three-dimensional orientations of structures and to determine formation thicknesses.

We used limb measurements to construct axial and described faults by recognizing sharp, juxtaposed contacts between units not in stratigraphic order, linear topographic breaks, and zones of calcite mineralization. We determined fault separation amount by constructing cross-sections. We measured orientations of exposed fault and related shear fracture surfaces and kinematic indicators such slickenlines and slickenfibers on fault surfaces.

Tectonic Setting

The map area is in a significant and complex area: the eastern margins of both the Cordilleran orogen and the Basin and Range province. Cretaceous sedimentary rocks in Sierra del Carmen were deposited in the easternmost Chihuahua trough, a basin connected to opening ancestral Gulf of Mexico (Muehlberger and Dickerson, 1989). Colliding plates along the western margin of North America created a broad deformation belt termed the Cordilleran orogen, whose youngest and easternmost part is termed the Laramide orogen (Fig 1; English and Johnson, 2004). From 70 – 50 million years before present (Ma) two phases of Laramide shortening deformed Cretaceous rocks in the Big Bend region (Fig. 1; Lehman, 1991). The first produced north– northwest trending folds and thrust faults, the second phase produced northeast-trending map scale folds (Cullen and others, 2013).

By 30 Ma much of the Cordilleran orogen began to extend, producing the Basin and

Range province. The initiation of a transform plate boundary, the San Andreas fault, collapse of over-thickened Cordilleran crust, and possibly mantle upwelling, triggered this extension. Basin and Range structures include mountain range-scale horst and graben structures bounded by normal faults and right-lateral strike slip faults. (Cobb and Poth, 1980; Moustafa, 1988). Basin and Range faulting continues today: the Big Bend region lies within the active Rio Grande rift and some faults in Sierra del Carmen cross-cut Quaternary and/or Tertiary gravels (Moustafa, 1988).

Later deformation phases likely took advantage of existing zones of weakness. As a result, Chihuahua trough-bounding normal faults may have been reactivated first as Laramide reverse faults and later as Basin and Range normal faults (Tauvers and Muhlberger, 1988).

Previous Work

Although several published geologic maps cover the northern Sierra del Carmen, our map area had not been mapped at a detailed, 1:12,000 scale. Tauvers and Muehlberger (1988) described Paleozoic rocks and Cretaceous cover at Persimmon Gap 15 km northwest of our map area. Geologic maps of Moustafa (1988; scale 1:48,000) and St. John (1966; scale 1:62,500) cover the mapping area. Ferrill and others (2004) and Smart and others (2010) described an extensional fault-propagation fold in Big Brushy Canyon. Cullen and others (2013) described polyphase folds and faults at Dagger Mountain in Big Bend National Park west the map area. Bailey Welch completed a 1:12,000-scale geologic map and described polyphase structures in Big Brushy Canyon directly to the north of this project area (Satterfield and Welch, 2014). Travis Williams completed a 1:12,000-scale geologic map and described structures in an area adjoining the project area to the west (Williams and Satterfield, 2015). An earlier version of the geologic map and figures in this paper were presented at the American Association of Petroleum Geologists Southwest Section 2015 Convention (Vera-Lopez et al., 2015).

KEY TO COMPILATION OF LARAMIDE STRUCTURES

Quaternary and Tertiary sediments

Tertiary volcanic rocks

Cretaceous - early Eocene sedimentary rocks

Underlain by shallow Paleozoic rocks (El Burro-Peyotes uplift)

Paleozoic sedimentary rocks exposed at surface

SE Dagger Mountain map area (Williams and Satterfield (2015) SW AAPG poster)

S Big Brushy Canyon map area (this paper)

Stairway Mtn - Big Brushy Canyon map area (Welch and Satterfield, 2014)

Dagger Mountain map area (Satterfield and others, 2014)

Fold; surface trace of axial plane; arrow shows dip direction of steep limb of monocline

Thrust fault; teeth on upper plate

High-angle reverse fault; box on upper plate

Left-lateral strike-slip fault

Boundary of Texas Lineament of Muehlberger (1980)

Place names

B	Boquillas, Coahuila, at head of Boquillas Canyon
C	Candelaria, TX
CM	Chisos Mountains
M	Marathon, TX
P	Presidio, TX
S	The Solitario
SDC	Sierra del Carmen
T	Terlingua, TX

Named Laramide structures

CDf	Chalk Draw fault
Ctb	Chihuahua tectonic belt
EBa	El Burro anticline
EBPu	El Burro-Peyotes uplift
FTm	Fresno-Terlingua monocline
LBf	La Babia fault
MMa	Mariscal Mountain anticline
Mu	Marathon uplift
SGa	Sierra Grande anticline
St	Santiago thrust
SVa	San Vicente anticline
Tmf	Tascotal Mesa fault

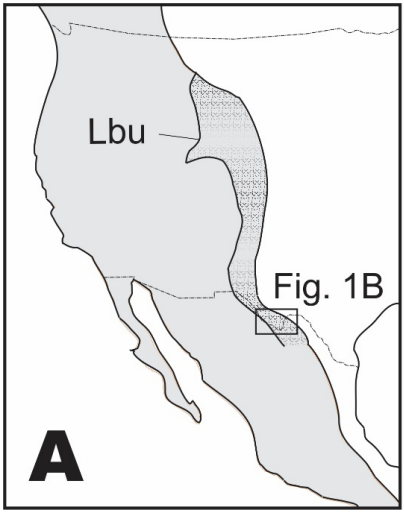

FIGURE 1A

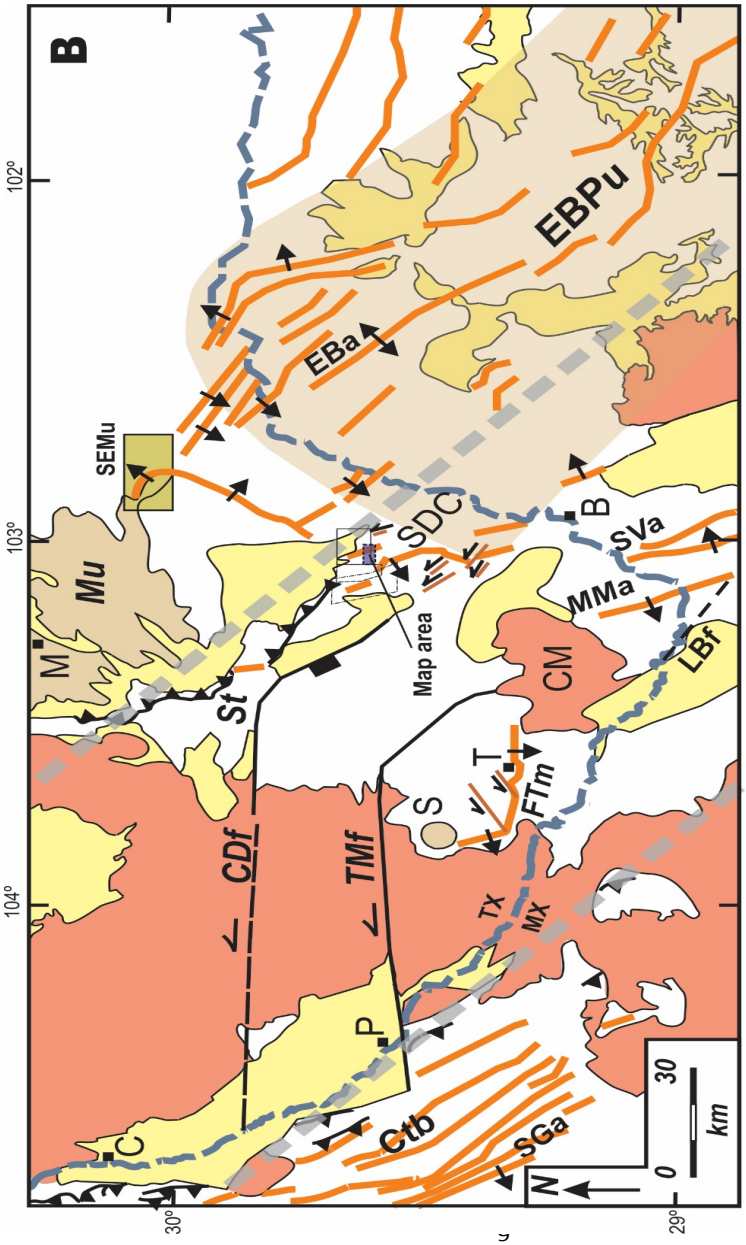

FIGURE 1B

Figure 1A & 1B. Structures of the Laramide orogen in the Big Bend region. (A) Tectonic map shows major folds, reverse faults, and left-lateral strike-slip faults of Laramide age, as well as locations of map areas mentioned in text. Map modified from Cullen and others (2013). Data sources given in Cullen and others (2013). (B) Map showing location of tectonic map, Cordilleran orogen (gray shade), and Laramide orogen basement uplifts (Lbu). Figure modified from Cullen and others (2013).

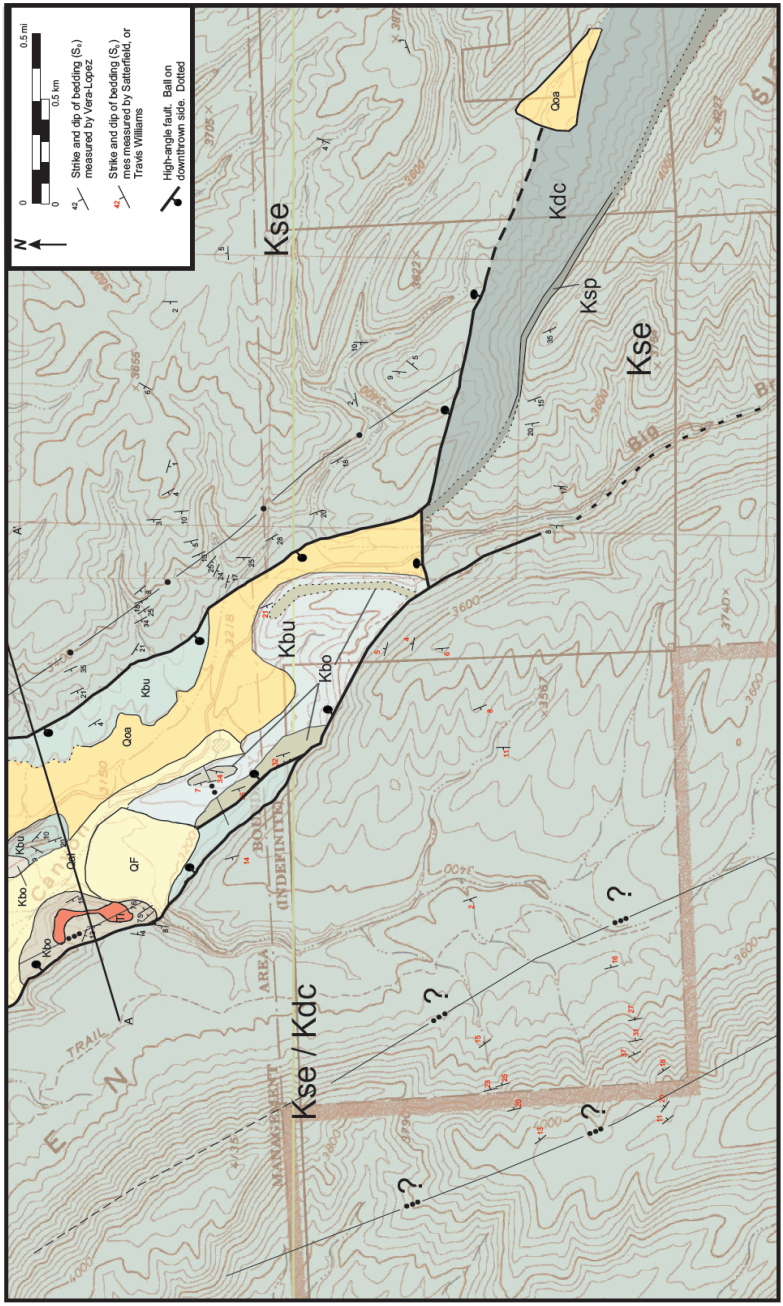

FIGURE 2

Figure 2. Geologic map of southern Big Brushy Canyon Area. Map shows map-scale D_1, D_2, and D_3 folds and cross-cutting relations between folds and D_3 high-angle faults. Monoclines identified with question marks could be D_3 folds or D_2 folds. Key to geologic map units in Table 1.

Period	Unit	Unit	Rock Type	Description
Quaternary	Alluvium	Qal	unconsolidated gravel, sand, and mud	Unconsolidated sediment found in recently active stream channels. Identified on aerial photographs by deep channels in valley floors and bright white color.
Quaternary	Alluvial fan deposits	Qf	unconsolidated gravel, sand, and mud	Poorly sorted, caliche cemented gray-tan conglomerate containing subrounded gravel sized clasts of limestone and chert. This unit is found where drainage from the fault blocks meets the flat ground. This unit is cross-cut by younger alluvial channels
Quaternary	Older Quaternary alluvium	Qoa	unconsolidated gravel, sand, and mud	Unconsolidated gravel found in older stream channels. The gravel is composed of various eroded limestone units. Identified on aerial photographs by flat topography with a light gray-tan color. Higher elevation than active channels
Tertiary	Tertiary intrusions	Ti	sill	Red-Brown slope-former mafic sills that intrudes the Boquillas Formation. This unit can be easily broken and displays spheroidical weathering.
Upper Cretaceous	Boquillas Formation	Kbo	Limestone and Shale	Cuesta-forming lime mudstone. White-tan in color, weathers to yellow-brown. Near intrusive sills, the color can be gray and orange. *Inoceramus* bivalves common. First-phase Laramide (D_1) folds are common in this unit.
Lower Cretaceous	Buda Limestone	Kbu	Limestone and marl	Upper: Ridge-forming oolitic wackestone. White in color, weathers to white-tan. Bivalve fossils present. Middle: Slope forming marl. Light gray to white in color. Weathers to small nodules. Lower: Ridge forming calcarenite. Red-tan in color, weathers to red-brown. Contains angular to sub-angular grains of 95% calcite and 5% rock fragments in a calcite matrix. Grain sizes around 1mm.
Lower Cretaceous	Del Rio Clay	Kdr	Mudstone and sandstone	Red-orange slope former, *Cribratina* foraminifera common in fine sandstone
Lower Cretaceous	Santa Elena Limestone	Kse	Limestone	Thick-bedded limestone, locally weathers light grey, Chert nodules, Scooped shaped bivalves within fossiliferous area, Thick bedded limestone, Petroliferous smell when broken , Round chert nodules, Rudist fossils
Lower Cretaceous	Sue Peaks Formation	Ksp	Limestone and Shale	Slope-former; Upper- thin bedded limestone, Lower- yellow/grey shale
Lower Cretaceous	Del Carmen	Kdc	Limestone	Thick-bedded limestone, Locally weathers dark brown, cliff former, elongate chert nodules along bedding planes

TABLE 1

Table 1. Key and descriptions of geologic map units on geologic map of southern Big Brushy Canyon Area.

Geologic Map Units

Geologic map units provide form surfaces for folds and help locate faults at breaks in expected stratigraphic order. Map unit ages constrain timing of folding and faulting. Our geologic map (Figure 2) distinguishes six Cretaceous geologic map units (Del Carmen Limestone, Sue Peaks Formation, Santa Elena Limestone, Del Rio Clay, Buda Limestone, and Boquillas Formation), Tertiary mafic sills intruding the Boquillas Formation, and three map units composed of Quaternary sediments. Table 1 gives detailed map unit descriptions. This section summarizes how geologic map units are distinguished from each other.

The oldest unit exposed within the map area, the Del Carmen Limestone (Kdc) consists of medium-gray-weathering, very thick-bedded, cliff-forming limestone that locally contains distinctive dark brown elongate chert nodules parallel to bedding planes (Maxwell et al., 1967). The overlying Sue Peaks Formation contains poorly exposed, slope-forming marl. The Santa Elena Limestone (Kse), which overlies the Sue Peaks Formation, consists of medium-gray-weathering, very thick-bedded, cliff-forming limestone (Fig. 3) containing distinctive somewhat equant chert nodules not in bedding planes (Maxwell et al., 1967). Santa Elena limestone beds have a possibly distinctive petroliferous smell when freshly broken (Moustafa, 1988). The overlying Del Rio Clay (Kdr) is a dark brown-red-colored slope-former exposed in Big Brushy Canyon just north of the map area. The overlying Buda Limestone (Kbu) consists of three distinctive members not distinguished on the map: lower red-brown weathering cliff-forming limestone, middle slope-forming marl, and upper white-light tan-weathering ridge forming limestone The Boquillas Formation, which overlies the Buda Limestone, contains distinctive, brown-weathering thin crystalline limestone and interbedded shale beds containing *Inoceramus* bivalves (Maxwell et al., 1967). Mafic Tertiary sills (Ti) intrude the Boquillas Formation.

In several fault blocks thick-bedded cliff-forming limestone can only be mapped as Del Carmen Limestone or Santa Elena Limestone (Kse/Kdc) because the distinctive map units above or below Kdc and Kse are not exposed and distinctive chert nodules have not been found.

Three Quaternary map units (Qal, Qf, and Qoa) contain unconsolidated gravel, sand, and mud and are distinguished by their surface topographic expression seen on stereo aerial photographs and in the field. Older alluvium (Qoa) form broad, relatively flat valleys cross-cut by deeper active stream channels containing younger alluvium (Qal). Alluvial fan deposits (Qf) are fan-shaped accumulations of sediments at mouths of large draws at range fronts.

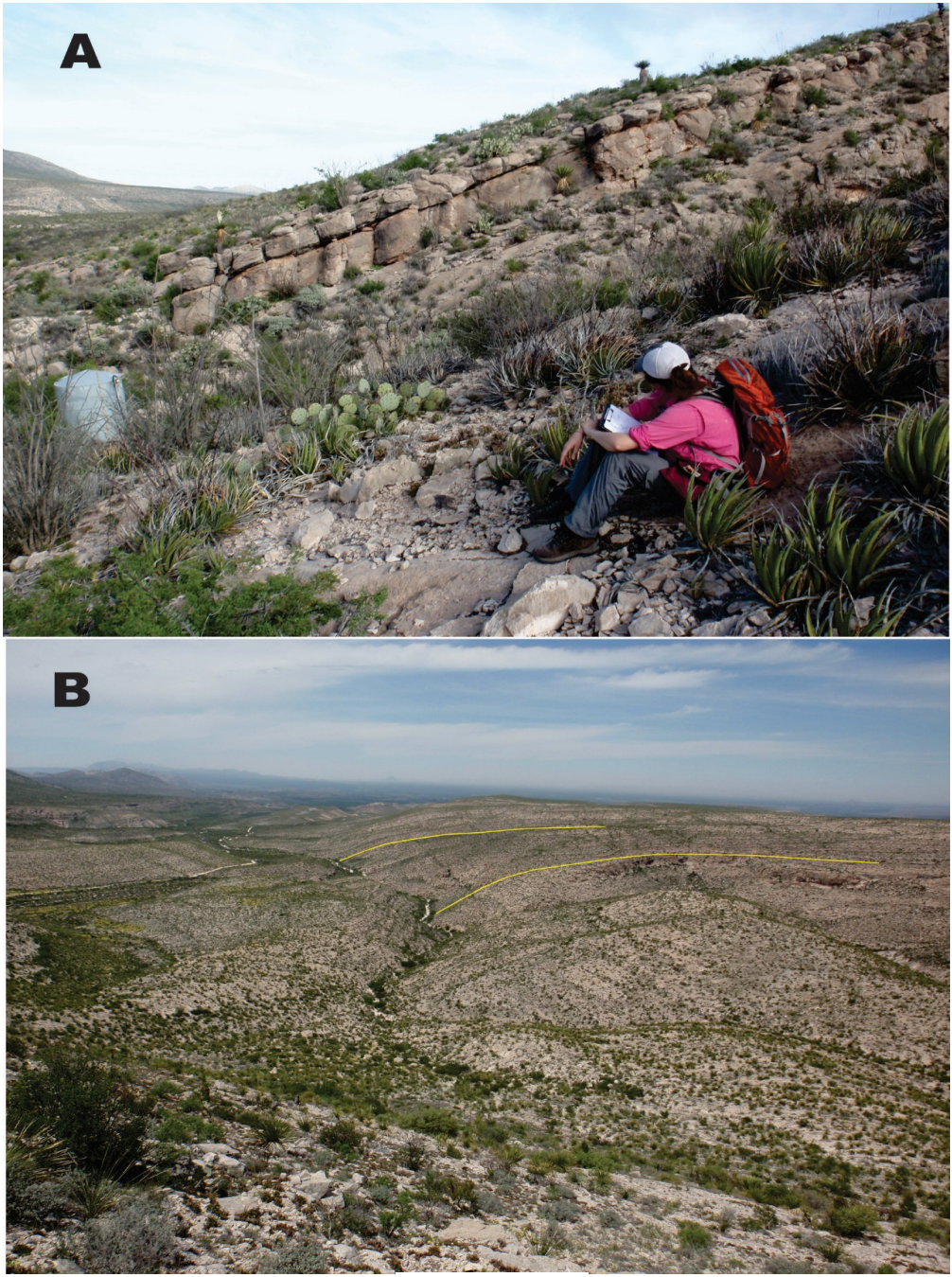

FIGURE 3

Figure 3. Photographs of a well-exposed Laramide (D1) monocline in map area. A northwest-striking Basin and Range high-angle fault cross-cuts this fold. (A) Steep

limb showing Santa Elena Limestone. This monocline is number 7 on stereographic projections. (B) View to northwest of same monocline. Northwest-trending high-angle Basin and Range fault is located in straight northwest-trending draw in center of photo.

Structures

The map area exposes three phases of map-scale folds and one phase of faults. Cross-cutting relations within the field area and in nearby locations in the northern Sierra del Carmen allow timing between deformation events to be documented. Map-scale D_1 folds are monoclines, folds which display a single steeply-dipping limb adjacent to gently-dipping limbs (Figs. 2, 3). Second-phase (D_2) folds refold both limbs of first-phase D_1 monoclines, producing gentle, 1 – 3 km-half-wavelength flexures best seen in Big Brushy Canyon to the north of map area (Satterfield and Welch, 2014). High-angle third-phase (D_3) faults cross-cut D_1 folds (Figs. 2, 4). D_3 faults strike north-northwest and northwest (Satterfield and Welch, 2014) and form the Big Brushy Canyon graben (Moustafa, 1988; Fig. 2). Map-scale D_3 folds are north-northwest- and northwest-striking monoclines. Several lines of evidence indicate that D_3 folds formed at the same time as high-angle D_3 faults: a) some D_3 folds are directly adjacent to D_3 faults, b) geometries of some D_3 folds are consistent with folds produced by drag during fault movement (Figs 2, 4), and c) to the north of the map area in Big Brushy Canyon one unusually well-exposed D_3 fold described by Ferrill and others (2004) and Smart and others (2010) drapes above the upper termination of a D_3 fault, characteristic of a extensional fault-propagation fold.

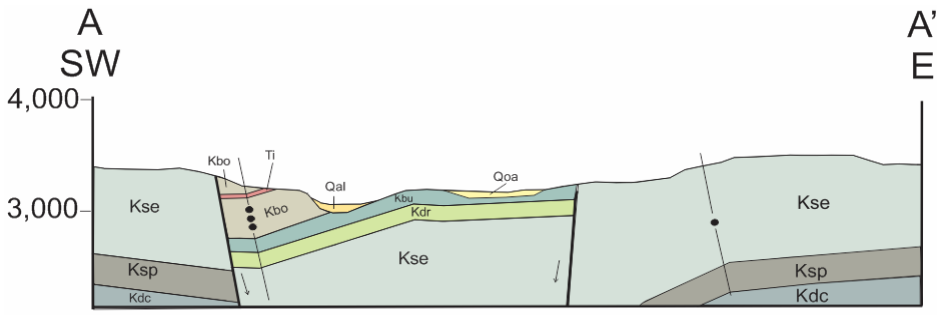

FIGURE 4

Figure 4. Cross section A – A'. No vertical exaggeration. Location shown on geologic map. The D_3 fold on the SW end is a drag fold caused by normal offset on the SW Basin and Range fault propagation folds because these deformation events caused structures of the same orientation. The fold on the NE end of the section is interpreted to be a Laramide fold (D_1) because it is cross-cut at a high angle by a Basin and Range (D_3) high – angle fault.

Stereographic projections (Fig. 5) help distinguish folds formed in three deformation events (D_1, D_2, and D_3). Techniques used to describe folds include: plotting strike and dips of fold limbs and constructing axial planes, fold axes, and interlimb angles on stereonets. First-phase (D_1) folds contain axial planes that average 332 85NE, fold axes that average 327 45, and an average interlimb angle of 52° (Fig. 5). Second-phase (D_2) folds contain axial planes that average 074 90, fold axes that average 254 8, and an average interlimb angle of 166°. Third-phase (D_3) folds, caused by high-angle D_3 faults, contain axial planes that average 322 64W, fold axes that average 322 10, and an average interlimb angle of 92°.

Two northwest-striking map-scale monoclines have orientations similar to first-phase and third-phase folds and lack cross-cutting relations with D_1 – D_3 folds and faults. These monoclines and others outside the map area cannot be identified as D_1 or D_3 folds with surface data.

Phase	Fold	Limbs	Interlimb angle	Axial plane	Fold Axis
D_1	7-1	1, 2	72°	328 58E	140 20
	7-2	3, 4	52°	314 74W	138 28
	5	1, 2	26°	302 82E	304 4
D_2	3	1, 2	166°	076 90	254 8
	7-1	1, 2	183°	058 86E	056
	7-2	2, 3	144°	068 90	066 18
D_3	2	1, 2	92°	332 64W	317 10
	1	1, 2	152°	357 84E	177 3
D_1 or D_3	6-1	1, 2	30°	343 88W	343 4
	6-2	2, 3	16°	358 84W	356 4
	4	1, 2	165°	334 70E	334 4

FIGURE 5

Figure 5. Stereographic projections of map-scale and outcrop-scale folds. Key to symbols: dot- pole to original bedding (S0), light grey band- average axial plane orientation, circle-dot- fold axis, and triangle-dot- pole to axial plane. Stereographic projections show fold axis and axial plane orientations alone can be used to distinguish D1 from D2 folds, but not D1 from D3 folds.

Conclusions and Sequence of Events

Our mapping combined with our understanding of regional tectonic events best supports this sequence of structural events:

1) D_1 folding produced relatively tight map-scale monoclines and folds in the Boquillas Formation that strike north-northwest and display subvertical axial planes. D_1 monoclines are interpreted to be contractional fault propagation folds above unexposed reverse faults. These structures are characteristic of flanks of Laramide basement uplifts in the easternmost Cordilleran orogen (e.g. Mitra and Mount, 1998).

2) D_2 folding produced gentle northeast-striking flexures that contain subvertical axial planes. D_2 folds are interpreted to be a second phase of Laramide shortening caused by a change in plate convergence direction.

3) D_3 high angle faulting produced adjacent and overlying north-northwest- and northwest-striking D_3 monoclines containing subvertical axial planes. D_3 folds are drag folds and extensional fault propagation folds interpreted to form during Basin and Range extension.

4) D_3 faults locally cross-cut older alluvium of Quaternary age (Figs 2, 4; Satterfield and Welch, 2014) documenting that some northern Sierra del Carmen Basin and Range faults are active.

D_1 and D_3 monoclines have very similar orientations and cannot be distinguished by orientation alone. Similar orientations of different fold phases results when Basin and Range extension likely reactivated D_1 faults. Extensional D_3 monoclines may be widespread and confused with contractional D_1 monoclines.

References

Cobb, R.C., and Poth S., 1980. Superposed deformation in the Santiago and Northern Del Carmen Mountains, Trans-Pecos Texas. New Mexico Geological Society Guidebook, 31st Field Conference, Trans-Pecos Region, p. 71 - 75.

Cullen, J., Knox, N.K., Crouch, J., and Satterfield, J.I., 2013: Polyphase Laramide Structures and Possible Folded Tertiary(?) Sills at Dagger Mountain, Big Bend National Park, Texas: The Compass: Earth Science Journal of Sigma Gamma Epsilon, v. 85, Available at: http://digitalcommons.csbsju.edu/compass/vol85/iss3/3

English, J., and Johnston, S., 2004. The Laramide Orogeny: What were the Driving Forces? International Geology Review, v. 46: p. 833 – 838.

Ferrill, D.A., Sims, D.W., Waiting, D.J., Morris, A.P., Franklin, N.M., Schultz, A.L., 2004, Structural framework of the Edwards Aquifer recharge zone in south-central Texas: Geological Society of America Bulletin, v. 116, p. 407-418.

Lehman, T.M., 1991, Sedimentation and tectonism in the Laramide Tornillo basin of West Texas: Sedimentary Geology, v. 75, p. 9 – 28.

Maxwell, R.A., Lonsdale, J.T., Hazzard, R.T., and Wilson, J.A., 1967. Geology of Big Bend National Park, Brewster County, Texas. Bureau of Economic Geology Publication 6711, Austin, Texas, 320 p., map scale 1: 62,500.

Mitra, S., and Mount, V.S., 1998, Foreland basement-involved structures: American Association of Petroleum Geologists Bulletin, v. 82, p. 70 – 109.

Moustafa, A.R., 1988. Structural geology of Sierra del Carmen, Trans – Pecos Texas. Bureau of Economic Geology Geologic Quadrangle Map No. 54, 28 p., map scale 1:48,000.

Satterfield, J.I., and Welch, B.L., 2014, Folded sills and fault-propagation folds in northern Sierra del Carmen, Big Bend region, Texas *in* Lampman, D., and Fitzgerald, H., eds., Hunting the Permian in the Permian basin, West Texas Geological Society Fall Symposium abstracts, p. 87 – 88.

Smart, K.J.,Ferrill, D.A., Morris, A.P., Bichon, B.J., Riha, D.S., Huyse, L., 2010, "Geomechanical modeling of an extensional fault-propagation fold: Big Brushy Canyon monocline, Sierra Del Carmen, Texas: American Association of Petroleum Geologists Bulletin, v. 94, p. 221-240.

St. John, B., 1966, Geologic Map of Black Gap Area, Brewster County, Texas: Bureau of Economic Geology Geologic Quadrangle Map No. 30, 18 p., map scale: 1:62,500.

Tauvers, P.R., and Muehlberger, W.R., 1988. Persimmon Gap in Big Bend National Park, Texas: Ouachita facies and Cretaceous cover deformed in a Laramide overthrust, *in* Hayward, O.T., ed., Centennial Field Guide v. 4, South – Central Section of the Geological Society of America, Geological Society of America, Boulder, Colorado, p. 417 – 422.

Vera-Lopez, L.V., Welch, B.L., and Satterfield, J.I., 2015, Map-scale folds in Big Brushy Canyon, Northern Sierra del Carmen, Big Bend Region, Texas: American Association of Petroleum Geologists Southwest Section 2015 Convention abstracts.

Williams, T.A., and Satterfield, J.I., 2015, Possible Cretaceous growth-faulting and a Laramide detachment in northern Sierra del Carmen, Big Bend region, Texas: American Association of Petroleum Geologists Southwest Section 2015 Convention abstracts.

Acknowledgements

Angelo State University awarded an Undergraduate Faculty-Mentored Grant which provided research funds to Laiza V. Vera-Lopez and Travis A. Williams. Angelo State University also provided Undergraduate Research Travel Funds so that Vera-Lopez and Williams could present results of this project at the American Association of Petroleum Geologists Southwest Section 2015 Convention in Wichita Falls. The Southwest Section of the American Association of Petroleum Geologists awarded a research grant to Bailey L. Welch. Big Bend National Park provided access and a research permit.

Black Gap Wildlife Management Area provided access, a research permit, and lodging. Mr. Travis Smith, Texas Parks and Wildlife Department, was especially helpful. Mr. Lyndell Shackelford provided access to the Shackelford Ranch. Mr. John Miller and Mr. Travis Potter, Stillwell Ranch, supported our work during stays at the Stillwell RV Park. Travis Williams and Sean Czarnecki assisted in mapping.

Using Areas of Concentrated *E. coli* Bacteria to Identify Species Specific Sources in Urbanized Sections of the Concho River, Tom Green County, Texas

Darren Seidel and James W. Ward, PhD, P.G.

Abstract

Seasonality has been shown to play an extremely responsible role in the fluctuation of Escherichia coli (*E. coli*) loading on the Concho River System in San Angelo, Texas. However even with temperature change and other physicochemical parameters varying with seasonal change, several sites exceed EPA's "safe versus unsafe for contact" surface water standard by three to ten times the respected < 320 colony forming units per 100 mL standard threshold value (at 3%). The objective of this project is to quantify areas of *E. coli* loading to further understand local sources of bacteria pollution. Ten sites located along highly urbanized sections of the Concho River will be sampled for *E. coli* and physiochemical properties including temperature, dissolved oxygen, specific conductance, conductance, total dissolved solids, and pH. The data set will encompass twenty-six sampling periods spread out over a year. The *E. coli* data was used to isolate areas where Bacteroides identification DNA markers which was sampled for birds, humans, and dogs. This project gives way to putting a numerical and biological answer to pollution of an urbanized surface water system with located within the area of interest.

*****

Introduction

Urbanization and human influenced alteration may negatively impact environmental quality and sustainability of surface water systems throughout the world. Continuous research is discovering new detection methods and means of expressing how impactful human and/or animal influences truly are on surface water systems. With the elevated risk of humans contracting pathogen-illness from surface water systems, a serious health related concern becomes evident when a surface water system becomes 303(d) impaired (TCEQ 2013). The Concho River in Concho and Tom Green Counties in west central Texas has been listed as a 303(d) impaired surface water system for two parameters (dissolved oxygen and bacteria) since 2008. Following the 2008 Texas Commission on Environmental Quality integrated report, the Concho River has been researched by local and regional based water science entities to understand where, what, and how the system is being altered and consequently impaired. *E. coli* bacteria has served as a water quality indictor for decades (Edberg 1988). Along with technological advancements, the accuracy and precision at

which *E. coli* bacteria is quantified is becoming better and better every year. Bacteroides bacteria are the most ideal fecal source tracking target for this experiment for several key reasons. Although Bacteroides and *E. coli* are quite similar, they don't express the same intestinal activities in a warm blooded animal. For that reason, Bacteroides function as bacterium that aid in nutrient absorption in the host and whatever the host species' food consumption is, allows for different gene profiles separating certain species from one another from a microbial standpoint (Coakley 2011, Hooper et al. 2001). However, only in recent years has a DNA based approach become regularly utilized to analyze specie specific hosts of contamination. With an extremely wide variety of physicochemical parameters, seasonality flux, and both point and non-point sources pollution impacting the Concho River, the focus of this research project is locating areas where *E. coli* bacteria is the most concentrated and using those sampling sites to conduct DNA based source host analysis. The objective of this project is to determine host specific data in order to transition a possible non-point source of contamination to a point source and then develop best management practices to low the possible contaminant sources to a "safe for contact" standard.

Project Statement: Previous research and analysis has determined the Concho River is subject to high levels of fecal coliform bacteria and specifically *E. coli* year around. Traditional analysis of *E. coli* bacteria shows a direct relation will temperature change. However, at certain localities of the Concho River within the city limits of San Angelo, Texas *E. coli* bacteria remains at a very high level regardless of temperature change, an excess of 2419.6 cfu/100 mL. Thus, the idea of possibly one or several year around contamination sources are impacting the system and leading to excessively high *E. coli* bacteria results. Therefore, the project aims to document the possible source of contamination and restore the Concho River to a non-impaired surface water statue. The Concho River is a valuable resource for eleven counties within the river's watershed and a large sub-basin of the Colorado River basin that stretches through the heart of the state of Texas.

Hypothesis: Fecal coliform and *E. coli* concentrated areas have one or several direct DNA based Bacteroides hosts contributing to the high levels of contamination found at two specific sites of interest in the research area.

Objective #1: **Quantify locations of *E. coli* loading at ten different sampling sites**

Task #1: Collect biweekly *E. coli* samples to isolate areas of high contamination load.

Task #2: Collect and document physiochemical data at each site per *E. coli* sample

Task #3: Document human, bird, and animal activity at each site during sampling

Objective #2: **Conduct DNA based sampling at highly contaminated sites**

Task #1: Collect samples using Source Molecular Corporation's procedures and

protocols for Bacteroides analysis for human, bird, and dog specific DNA markers
Task #2: Aid in creating best management practices to lower negative environmental impact on the Concho River upon results from Source Molecular Corporation Laboratory

The Concho River: Location, Geology, and Impact

The Concho River is regionally broken into three major watershed contributories; North, Middle, and South Concho Rivers. All three major contributories meet near the Bell Street Dam located within the city limits of San Angelo, Texas (Figure 1). The Concho River Basin as a whole encompasses eleven Texas counties and runs into Lake O.H. Ivie (Smith 2015, LCRA 2008) all while supplying essential water sources to families, farmers, and ranch near the river system.

The North Concho River – is a highly variable watershed of the Concho River that extends from northcentral Glasscock County to O.C. Fisher Reservoir. Although the watershed extends through a large portion of the Concho River basin, the North Concho River remains dry though most of the year.

The Middle Concho River – is a west to east contributory to the Concho River basin that extends as far west as central Upton County. Much like the North Concho River, and with the exception of isolated spring contributions, the watershed remains dry throughout most of the year. The watershed extends to the north pool of Twin Buttes Reservoir.

The South Concho River – is a south to north contributory that offers continuous spring fed influence to the Concho River basin. Although many dams are located throughout the river system, it is the only branch of the Concho River that offers water flow year around. Flow continues through much of southern Tom Green County and extends to the south pool of Twin Buttes Reservoir.

All three watersheds are controlled by manmade reservoir structures that control the overall flow of the three watersheds prior to all three watersheds meeting at the Bell Street Dam (Henry 1986). From the Bell Street Dam, flow continues eastward to O.H. Ivie where the Concho River meets the Colorado River. Within the Concho River watershed, shallow, Permian aged aquifers contribute upwelling sources of groundwater in isolated locations (Dutton et al. 1989).

The lithological influences on the Concho River Basin mostly consist of Cretaceous-age carbonates with a small area of Permian aged sandstones and conglomerates near the convergence of the three watersheds (UCRA, 2011). The Cretaceous-age carbonates found at the surface throughout the Concho River Basin are subject to many secondary structures such as joints and karstic type conduits and vugs (Henderson 1928, Orndorff et al. 2001, Craig 1988).

Many rural communities rely on irrigation and other agricultural activities to be supplemented from water use out of the Concho River. Large cotton, milo, and other cash crops are grown within the Concho River Basin and in Tom Green County alone

956,852 acres exist in farm production (USDA 2012). Consequently, the more negatively impacted the Concho River becomes upstream, the larger the possibility of adverse effects becoming evident downstream. Controlling human impact and developing large scale management practices will help control the contamination within urbanized sections of the Concho River in San Angelo, Texas and consequently downstream.

Methodology and Experimentation

The twenty-six biweekly sampling period as directed in the Quality Assurance Project Plan (QAPP) began on May 8, 2014 with the first round of *E. coli* sampling. The collection period for *E. coli* extended through April 29, 2015. All physiochemical parameters were taken using a pre and post calibrated Professional Series Yellow Spring Instrument Multi-Parameter Aquatic Sampling Soude and calibrated under United States Geological Survey calibration protocols (Wagner et al. 2006). These physiochemical parameters included; water temperature and pressure, dissolved oxygen levels (% and mL), specific conductance, conductance, total dissolved solids, and pH. *E. coli* collections were done using the IDEXX Laboratories' Colilert Procedures (2013, Eaton et al. 2005). Upon collection of parameters and *E. coli* samples, the visible environmental conditions were documented and described in a field notebook. This information included: bird and other animal activity, human activity, water color and odor, trash and debris, and prior weekly precipitation. No sample collection period was conducted prior to a thirty-six hour buffer time period after a local rain event. The IDEXX Colilert method is a process at which a 100 mL of sampling media is collected from a site of interest to generate a most probable number of colony forming units per 100 mL to represent the *E. coli* level at the site (cfu/100 mL). Similar experimentations have been conducted on other surface water systems in a regional proximity such as the Rio Grande River (Mendoza et al. 2004), along the Kentucky River (Black et al. 2007), and as far away as Sweden (Novel, Novel 1976) making the Colilert method a local, regional, and internationally recognized method used for quantifying *E. coli*. As directed in the QAPP, no dilution or duplications were conducted because the main objective was to locate the areas with the most consistently high *E. coli* measurements in order to collect the sites for future DNA based Bacteroides analysis.

Results

After completion of the final *E. coli* sampling period on April 29, 2015, a twenty-six sample baseline was created with averages of all ten research sampling sites. The ten sampling sites and the associated *E. coli* (cfu/100 mL) values are as follows: Site 1 – 151.7, Site 2 – 190.0, Site 3 – 64.4, Site 4 – 776.3, Site 5 – 399.8, Site 6 – 181.6, Site 7 – 58.2, Site 8 – 1525.9, Site 9 – 364.3, Site 10 (was only sampled three times, no water present). In order to understand the severity of *E. coli* contamination, the data was compared to the Recommendation 2 criteria element for the statistical threshold value

for *E. coli* in fresh water, 320 cfu/100 mL. Recommendation 2 was developed by the Environmental Protection Agency in 2012 when the federal entity released the 2012 Recreational Water Quality Criteria (RWQC) recommendations (EPA 2012). The standard expresses an estimated illness rate of 32/1,000 (3.2%) which approximates the 90th percentile of water quality distribution and is intended to be a value that should not be exceeded by more than 10% of samples analyzed. When coupling this analysis with data from the Concho River sampling baseline, two sites, Site 4 and Site 8, exceed the 320 cfu/100 mL correlation valve by 2.426 times and 4.768 times, respectively.
After deliberation, research stakeholders concluded that sampling Site 4 and Site 8 for Human, Dog, and Bird Fecal detection would be the most conducive means of isolating species specific sources of contamination. Physical presents of all three hosts were documented consistently at these localities. At Site 4 and Site 8, respectively, an average bird population of ≈25 and ≈35 birds were counted and documented during the sampling period. Numerous samplings at Sites 4 and 8 were also conducted with heavy human traffic and an occasional dog(s) present. On June 11, 2015, the first round of DNA based sampling was conducted by Mr. Chuck Brown of the Upper Colorado River Authority and analyzed by Source Molecular Corporation in Miami, Florida on June 22, 2015. All three host analysis came back negative. Site 4 and Site 8 were collected and analyzed for two Human Bacteroidetes ID™ Species; Bacteroides dorei. B and EPA Developed Assay biomarkers, one Bird Fecal ID™; genus Helicobacter (classified as genus Campylobacter prior to 1989), and one Dog Fecal ID™; Dog Bacteroidetes.

Discussion

The results of the Bacteroides sampling when compared to the *E. coli* baseline averages offers an interpretation and possible an environmental factor as well. Between the last sampling period for *E. coli* and the first Bacteroides sampling, according to the National Weather Service, Tom Green County alone received 9.12 inches of rainfall. In one month, Tom Green County almost received half of the county's annual rainfall total (Henderson 2010). Thus a possible interpretation of the negative Bacteroids bacteria could be a result of a natural "flushing" of the surface water system through massive storm water run-off. Comparatively to *E. coli*, Bacteroids bacteria are the most numerous intestinal bacteria and encompass as my as 1,011 cells per gram of dry fecal matter (Coakley 2011, Finegold et al. 1983). The baseline data set of *E. coli* sampling reflects a large number of *E. coli* cfu/100 mL regardless of temperature fluctuation. Therefore, if year around *E. coli* bacteria are documented at a site, Bacteroids bacteria should be within that same area and be environmentally impacting a water system as well.

The *E. coli* data also revealed some interesting information in regards to sites with low *E. coli* bacteria counts. Site 3 and Site 7 are located in two very different places on the Concho River and both exhibit low *E. coli* averages (64.4 and 58.2 cfu/100

mL) consistently throughout the project timeline. Site 3 was sampled at the middle of the Bell Street Dam structure and was the only site that had a continuous year around discharge from a drain pipe located in the middle of the structure and controlled by the City of San Angelo. Site 7 is the furthest upstream site located on the newly remediated Concho River Trail in downtown San Angelo. Both sites are located directly downstream from the two most polluted sites along the river and show very different correlations to their polluted counterparts: Site 3 vs. Site 4 (64.4 - 776.3 cfu/100 mL) and Site 7 vs. Site 8 (58.2 - 1525.9 cfu/100 mL).

Conclusion

The high points of *E. coli* sampling show a strong relation in variation when comparing them to the low points of *E. coli* sampling in a relatively short distance. Could the dam structures in between site locations be serving as impediments to the surface water system's nature flow and consequently variation in bacteria populations? How long can the bacteria polluting the river survive under nature conditions? Even though there were two different bacteria of interest in this research, the project gives way to areas that have been documented with high *E. coli* values but still have an unknown DNA based analysis of the pollution as to where the pollution is coming from. Although the Bacteroides sampling was not conducive of any species specific data for the contamination, it did give rise to how the Concho River can exhibit a return to a low bacteria count river system after a strong influence of rain. This could have made the system reflect a more "nature" flow pattern even with dam structures throughout the river. In order to apply some of these ideas to the research, future work in creating a larger baseline of *E. coli* data at each site and further sampling of Bacteroides primers/markers at the most contaminated sites could offer the proper explanation to exactly what is contaminating the Concho River and the most effective means of remediation to control the contamination.

Table 1: *E. coli* sampling results (cfu/100 mL)

		Site #1	Site #2	Site #3	Site #4	Site #5	Site #6	Site #7	Site #8	Site #9	Site #10
	Bacteria										
5/9/2014					980.4	>2419.6	79.4		>2419.6	261.3	N/A
5/22/2014		920.8	410.6	110.6	>2419.6	1413.6	163.1	10.7	1046.2	16.9	N/A
6/7/2014		11	5.2	10.9	488.4	43.9	121.1	10.6	1299.7	36.8	95.9
6/21/2014		613.1	163.1	48.8	>2419.6	>2419.6	2419.6	57.6	>2419.6	>2419.6	>2419.6
7/2/2014		140.8	>2419.6	141.4	>2419.6	298.1	770.1	5.1	547.5	9.5	N/A
7/19/2014		6.2	34.5	16.3	325.5	435.2	27.8	7.2	>2419.6	>2419.6	N/A
8/5/2014		3.1	34.1	7.2	6.3	403.4	27.8	410.6	1046.2	1299.7	920.8
9/5/2014		8.5	117.8	6.2	2419.6	9.6	46.4	5.2	>2419.6	228.2	N/A
9/22/2014		920.8	648.8	260.3	1553.1	35.4	69.7	41.4	>2419.6	12	N/A
9/29/2014		7.5	5.1	18.1	19.3	8.3	46.5	16	>2419.6	28.1	N/A
10/20/2014		4.1	10.7	11.8	2419.6	547.5	34.5	11.8	>2419.6	11.9	N/A
10/27/2014		7.3	6.2	3	980.4	22.3	38.8	9.6	>2419.6	13.1	N/A
11/10/2014		156.5	88.6	145.5	547.5	325.5	172.2	123.6	>2419.6	298.7	N/A
11/20/2014		68.9	53	62	238.2	33.2	105.4	49.6	>2419.6	186	N/A
12/5/2014		39.3	35	128.1	547.5	151.5	43.5	23.3	1732.9	55.6	N/A
1/27/2015		35	27.2	23.5	62	14.8	29.2	8.5	166.4	80.9	N/A
2/1/2015		501.2	344.8	290.9	435.2	1413.6	140.1	248.1	866.4	410.6	N/A
2/10/2015		21.3	25.9	19.9	816.4	13.2	28.2	11	325.5	151.5	N/A
2/18/2015		15.8	17.1	18.9	32.3	22.3	10.8	12.2	152.9	44.8	N/A
2/23/2015		14.8	25.6	54.6	60.2	21.3	48.8	19.9	325.5	41	N/A
3/11/2015		16	6.3	3	30.7	115.3	45	3	275.5	44.8	N/A
3/25/2015		98.7	122.3	95.9	461.1	58.1	29.8	28.5	435.2	141.4	N/A
4/1/2015		27.5	15.3	9.8	103.6	28.8	9.8	18.3	1553.1	435.2	N/A
4/8/2015		43.5	13.5	8.4	30.3	18.1	9.5	36.9	2419.6	325.5	N/A
4/22/2015		69.5	83.6	64.5	328.2	84.2	152.9	222.4	866.4	172.7	N/A
4/29/2015		41.1	36.9	49.5	37.9	38.3	50.4	63.8	2419.6	325.5	N/A

Table 2: Bacteroides Analysis Results for Site 4 and Site 8

Results of Preliminary Interpretations of Fecal Pollution ID™					
Analysis Provider: Source Molecular Corporation					
Host of Interest	**Site Location**	**Date Received**	**Date Reported**	**Specie Analysis**	**DNA Analysis Result**
Human	4	11-Jun-15	22-Jun-15	*Bacteroides dorei*	Negative
Human	8	11-Jun-15	22-Jun-15	*Bacteroides dorei*	Negative
Human	4	11-Jun-15	22-Jun-15	EPA Developed Assay	Negative
Human	8	11-Jun-15	22-Jun-15	EPA Developed Assay	Negative
Bird	4	11-Jun-15	22-Jun-15	*Helicobacter*	Negative
Bird	8	11-Jun-15	22-Jun-15	*Helicobacter*	Negative
Dog	4	11-Jun-15	22-Jun-15	Dog *Bacteroidetes*	Negative
Dog	8	11-Jun-15	22-Jun-15	Dog *Bacteroidetes*	Negative

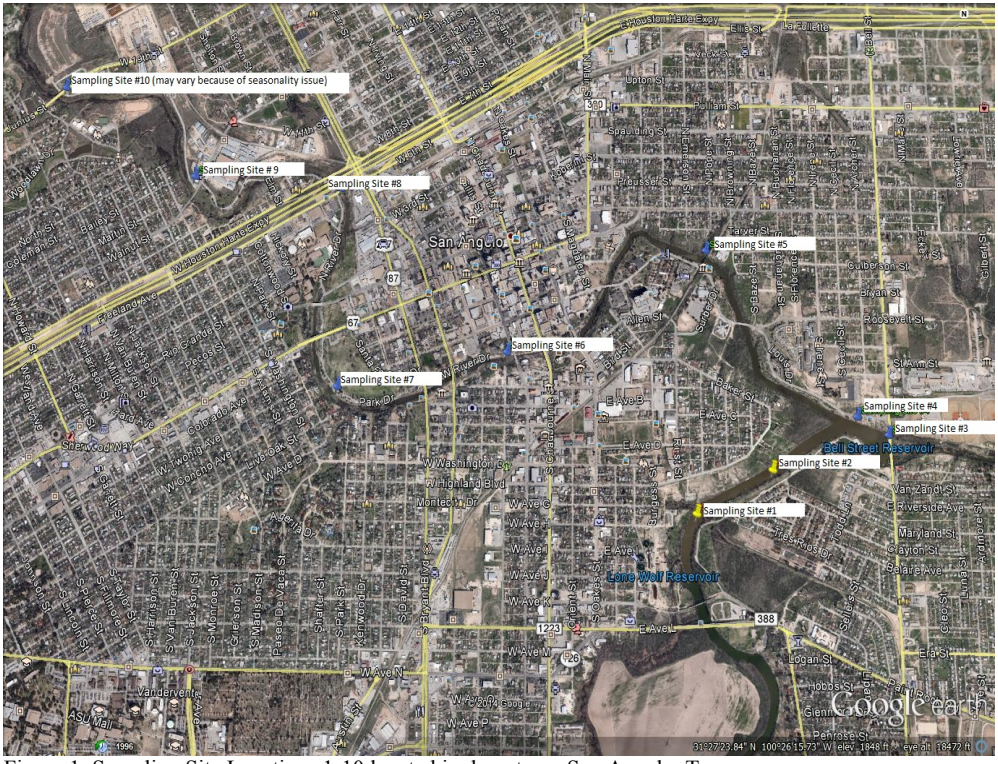

Figure 1: Sampling Site Locations 1-10 located in downtown San Angelo, Texas


Figure 2: Physiochemical Sampling at Site 5 (photo by Monique Ching, 2014)

References

1. Black, L.E., Brion, G.M., Freitas, S.J., 2007, Multivariate Logistic Regression for Predicting Total Culturable Virus Presence at the Intake of a Potable-Water Treatment Plant: Novel Application of the Atypical Coliform/Total Coliform Ratio, American Society for Microbiology, v. 73(12), p. 3965-3974.
2. Coakley, T.L., 2011, Locating Hot Spots of Human Fecal Pollution in an Urban Watershed of Central Kentucky Using Bacteroides 16S RRNA Markers, University of Kentucky Libraries, p. 6-9.
3. Craig, D.H., 1988, Caves and Other Features of Permian Karst in San Andres Dolomite, Yates Field Reservoir, West Texas, Paleokarst, p. 342-343.
4. Dutton, A.R., Richter, B.C., Kreitler, C.W., 1989, Brine Discharge and Salinization, Concho River Watershed, West Texas, Groundwater, v.27 (3), p. 375.
5. Eaton, A.D., Clesceri, L.S., Greenburg, A.E., Rice, E.N., Standard Methods for the Examination of Water and Wastewater, American Public Health Association, 2005, Washington, DC.
6. Edburg, S.C., Edburg, M.M., 1988, A Defined Substrate Technology for the Enumeration of Microbial Indicators of Environmental Pollution, The Yale Journal of Biology and Medicine, v. 61, p. 389-393.
7. Environmental Protection Agency, 2012 Recreational Water Quality Criteria, 2012, 4305T, EPA -820-F-12-061, Docket No. EPA-HQ-OW-2011-0466.
8. Finegold, S. M., Sutter, V. L., & Mathisen, G. E., 1983, Normal indigenous intestinal flora. Human intestinal microflora in health and disease, 1, 3-31.
9. Henderson, G.G., 1928, The Geology of Tom Green County, University of Texas Bulletin, No. 2807, p. 5-19.
10. Henderson, J.C ., 2010, "TOM GREEN COUNTY," Handbook of Texas Online, http://www.tshaonline.org/handbook/online/articles/hct07, Texas State Historical Association.
11. Henry, B.C., 1986, Mayflies (Ephemeroptera) of the Concho River, Texas, The Southwestern Naturalist, v. 31 (1), p. 15-16.
12. Hooper, L.V., Wong, M.H., Thelin, A., Hansson, L., Falk, P.G., Gordon, J.I., 2001, Molecular Analysis of Commensal Host Microbial Relationships in the Intestine, Science 2, v. 291 (5505), p. 881-884.
13. IDEXX Laboratories Inc., 2013, Colilert, 06-12999-06.
14. Lower Colorado River Authority (LCRA), 2008, Concho River Watershed Map.
15. Mendoza, J., Botsford, J., Hernandez, J., Montoya, A., Saenz, R., Valles, A., Vazquez, A., Alvarez, M., 2004, Microbial Contamination and Chemical Toxicity of the Rio Grande, BMC Microbiology, v.4 (17), p. 1-14.
16. Novel, M., Novel, G., Regulation of beta-glucuronidase synthesis in Escherichia Coli K-12: Constitutive Mutants Specifically Derepressed for uidA Expression, American Society of Microbiology, Journal of Bacteriology, v. 127 (1), p. 406-411.

17. Orndorff, R.C., 2001, Geologic Framework of the Ozarks of South-Central Missouri – Contributions to a Conceptual Model of Karst, U.S. Geological Survey Karst Interest Group Proceedings, Water-Resources Investigations Report, 01-4011, p. 18-19.
18. Smith, J.C., 2015, Concho River, Texas State Historical Association.
19. Texas Commission on Environmental Quality (TCEQ), 2013, 2012 Texas Integrated Report – Texas 303(d) List (Category 5), p. 75.
20. Upper Colorado River Authority, 2011, Concho River Protection Plan, Concho River, Watershed Advisory Board.
21. Wagner, R.J., Boulger, R.W., Oblinger, C.J., Smith, B.A., 2006, Guidelines and Standard Procedures for Continuous Water-Quality Monitors: Station Operation, Record Computation, and Data Reporting, U.S. Geological Survey Techniques and Methods, 1-D3, 51, p. 11-12.
22. United States Department of Agriculture (USDA), 2012, 2012 Census of Agriculture County Profile, Tom Green County, Texas, Census of Agriculture, v. 1.

Acknowledgements

Angelo State University Undergraduate (ASU) Research Fellowship – RAM Grant
Environmental Protection Agency Region 6 (South Central) (Urban Waters – UCRA Concho River Study; Title: Improving Water Quality Through Activities of the Concho River Basin Aquatic Education and Research Center)
ASU Department of Physics and Geosciences
Upper Colorado River Authority
United States Geological Survey
Dr. James W. Ward, ASU Department of Physics and Geosciences
Mr. Scott McWilliams and Chuck Brown, UCRA
Steve Shaw, First View Resources
Ms. Robin Cypher, Texas Commission on Environmental Quality (TCEQ)
Mr. Vaden Aldridge and Mr. Jarrett Louder